

A Novel Proportional Fairness Criterion for Throughput Allocation in Multirate IEEE 802.11

M. Laddomada, F. Mesiti, M. Mondin, and F. Daneshgaran

Abstract

This paper focuses on multirate IEEE 802.11 Wireless LAN employing the mandatory Distributed Coordination Function (DCF) option. Its aim is threefold. Upon starting from the multi-dimensional Markovian state transition model proposed by Malone *et.al.* for characterizing the behavior of the IEEE 802.11 protocol at the Medium Access Control layer, it presents an extension accounting for packet transmission failures due to channel errors. Second, it establishes the conditions under which a network constituted by N stations, each station transmitting with its own bit rate, $R_d^{(s)}$, and packet rate, λ_s , can be assumed loaded. Finally, it proposes a modified Proportional Fairness (PF) criterion, suitable for mitigating the *rate anomaly* problem of multirate loaded IEEE 802.11 Wireless LANs, employing the mandatory DCF option. Compared to the widely adopted assumption of saturated network, the proposed fairness criterion can be applied to general loaded networks.

The throughput allocation resulting from the proposed algorithm is able to greatly increase the aggregate throughput of the DCF, while ensuring fairness levels among the stations of the same order as the ones guaranteed by the classical PF criterion.

Simulation results are presented for some sample scenarios, confirming the effectiveness of the proposed criterion for optimized throughput allocation.

Index Terms

DCF, Distributed Coordination Function, fairness, IEEE 802.11, MAC, multirate, non-saturated, proportional fairness, rate adaptation, saturation, throughput, traffic, unloaded, unsaturated.

I. INTRODUCTION

Consider the IEEE802.11 Medium Access Control (MAC) layer [1] employing the DCF based on the Carrier Sense Multiple Access Collision Avoidance CSMA/CA access method. The scenario envisaged in this work considers N contending stations; each station generates data packets with constant rate λ_s by employing a bit rate, $R_d^{(s)}$, which depends on the channel quality experienced. In this scenario, it is known that the DCF is affected by the so-called *performance anomaly* problem [2]: in multirate networks the aggregate throughput is strongly influenced by that of the slowest contending station.

After the landmark work by Bianchi [3], who provided an analysis of the saturation throughput of the basic 802.11 protocol assuming a two dimensional Markov model at the MAC layer, many papers have addressed almost any facet of the behaviour of DCF in a variety of traffic loads and channel transmission conditions.

Contributions proposed in the literature so far can be classified in two main classes, namely *DCF Modelling* and *DCF Throughput and Fairness Optimization*.

Massimiliano Laddomada is with the Electrical Engineering Dept. of Texas A&M University-Texarkana, email: mladdomada@tamut.edu.

F. Mesiti and M. Mondin are with DELEN, Politecnico di Torino, Italy.

F. Daneshgaran is with ECE Dept., California State University, Los Angeles, USA.

DCF modelling. This is the topic that received the most attention in the literature since the work by Bianchi [3]. Papers [4]-[6] model the influence of real channel conditions on the throughput of the DCF operating in saturated traffic conditions, while [7]-[9] thoroughly analyze the influence of capture on the throughput of wireless transmission systems. Paper [10] investigates the saturation throughput of IEEE 802.11 in presence of non ideal transmission channel and capture effects. The behavior of the DCF of IEEE 802.11 WLANs in unsaturated traffic conditions has been analyzed in [11]-[18]. In [19], the authors look at the impact of channel induced errors and of the received Signal-to-Noise Ratio (SNR) on the achievable throughput in a system with rate adaptation, whereby the transmission rate of the terminal is modified depending on either direct or indirect measurements of the link quality.

Multirate modeling of the DCF has received some attention quite recently [20]-[24] as well. In [20] an analytical framework for analyzing the link delay of multirate networks is provided. In [21]-[22], authors provide DCF models for finite load sources with multirate capabilities, while in [23]-[24] a DCF model for networks with multirate stations is provided and the saturation throughput is derived. Remedies to performance anomalies are also discussed. In both previous works, packet errors are only due to collisions among the contending stations.

DCF throughput and fairness optimization. This is perhaps the issue most closely related to the problem dealt with in this paper. The main reason for optimizing the throughput allocation of the 802.11 DCF is the behaviour of the basic DCF in heterogeneous conditions, with stations transmitting at multiple rates: the same throughput is reserved to any contending station irrespective of its bit rate, with the undesired consequence that lowest bit rate stations occupy the channel for most time with respect to high rate stations [25]. Furthermore, the optimization of the aggregate throughput when different stations contend for the channel with different bit rates cannot be done without considering an appropriate fairness approach; the reason is that the optimum throughput would be achieved when only the highest rate stations access the channel [25]. In order to face this problem, a variety of throughput optimization techniques, which account for fairness issues, have been proposed in the literature. Paper [25] proposes a proportional fairness throughput allocation criterion for multirate and saturated IEEE 802.11 DCF by focusing on the 802.11e standard. In papers [26]-[29] the authors propose novel fairness criteria, which fall within the class of the time-based fairness criterion. Time-based fairness guarantees equal time-share of the channel occupancy irrespective to the station bit rate.

Paper [30] investigates the fairness issue in 802.11 multirate networks by analyzing various time-based fairness criteria. It demonstrates that with equal time-share of the channel occupancy among multirate stations, the throughput achieved by a reference station in a multirate scenario with N contending stations is equal to the throughput that the same reference station would achieve in a single rate scenario when contending with other $N - 1$ stations with its same rate. Furthermore, the authors prove that the proportional fairness criterion corresponds to fair channel time allocation in a multirate scenario.

The effect of the contention window size on the performance of the DCF have been also investigated in [31]-[33] in a variety of different scenarios. Finally, papers [34]-[39] have been devoted to the throughput optimization of the underlined DCF by optimizing a number of key parameters of the DCF, such as the minimum contention window size or the packet size.

A common hypothesis employed in the literature regards the saturation assumption, which sometimes does not fit quite well to real network traffic conditions. In real networks, traffic is mostly non-saturated, different stations usually operate with different loads, i.e., they have different packet rates, while the transmitting bit rate can also differ among the contending stations. Channel conditions are far from being ideal and often packet transmission has to be rescheduled until the data is correctly received. Due to Rayleigh and shadow fading conditions, a real scenario presents stations transmitting at different bit

rates, because of multirate adaptation foreseen at the physical layer of WLAN protocols such as IEEE 802.11b. In all these situations the common hypothesis, widely employed in the literature, that all the contending stations have the same probability of transmitting in a randomly chosen time slot, does not hold anymore.

The aim of this paper is to investigate the behaviour of the DCF in the most general scenario of a multirate network, when all the previous effects act jointly, as well as to present a proportional fairness criterion which accounts for general loading conditions as exemplified by the packet rate λ_s of the contending stations. Contrary to the aforementioned works available in the literature, we assume that the s -th station generates data packets with its own size, $PL^{(s)}$, with its own constant rate λ_s by employing a bit rate, $R_d^{(s)}$, which depends on the channel quality experienced, and it employs a minimum contention window with size $W_0^{(s)}$. Moreover, each station is in a proper load condition, which is independent from the loading conditions of the other contending stations. Notice that these hypotheses make the model proposed in this work quite different from the ones available in the literature, where the saturated condition is mostly adopted. One consequence of the proposed analysis is that unloaded, heterogeneous networks do not need any throughput allocation among stations. We propose a theoretical framework in order to identify whether a tagged station is saturated, given the traffic conditions of the remaining stations. As a starting point for the derivations that follow, we consider the bi-dimensional Markov model proposed in [12], and present the necessary modifications in order to deal with multirate stations, non ideal transmission channel conditions, and different packet sizes among the contending stations.

The rest of the paper is organized as follows. Section II provides the necessary modifications to the Markov model proposed in [12], while the employed traffic model is discussed in Section II-D. Section III proposes an analytical framework able to verify whether a network of N contending stations is loaded. The novel proportional fairness criterion is presented in Section IV, while Section V presents simulation results of some sample network scenarios. Finally, Section VI draws the conclusions.

II. THE NETWORK SCENARIO: OVERVIEW OF THE MARKOVIAN MODEL CHARACTERIZING THE DCF

In [12], the authors derived a bi-dimensional Markov model for characterizing the behavior of the DCF in heterogeneous networks, where each station has its own traffic, which could be finite and characterized by the parameter λ , expressing the packet arrival rate. In order to deal with non-saturated conditions, the traffic model is described by an exponentially distributed packet inter-arrival process. In this paper we consider a more general network than [12]. Indeed, in the investigated network, each station employs a specific bit rate, $R_d^{(s)}$, a specific transmission packet rate, λ_s , transmits packets with size $PL^{(s)}$, and it employs a minimum contention window with size $W_0^{(s)}$, which can differ from the one specified in the IEEE 802.11 standard [1] (these modifications are at the very basis of the proportional fairness criterion proposed in Section IV). A finite retry limit is considered in order to avoid infinite number of retries when bad channel conditions inhibit the station from successful transmission.

For the sake of greatly simplifying the evaluation of the expected time slots required by the theoretical derivations that follow, we consider $N_c \leq N$ classes of channel occupancy durations¹. First of all, given the payload lengths and the data rates of the N stations, the N_c duration-classes are arranged in order of decreasing durations identified by the index $d \in \{1, \dots, N_c\}$, whereby $d = 1$ identifies the slowest class. Notice that in our setup a station is denoted fast if it has a short channel occupancy.

¹This assumption relies on the observation that in actual networks some stations might transmit data frames presenting the same channel occupancy. As an instance, a station STA1 transmitting a packet of size 128 bytes at 1 Mbps occupies the channel for the same time of a station STA2 transmitting a packet of size 256 bytes at 2 Mbps.

Furthermore, each station is identified by an index $s \in \{1, \dots, N\}$, and it belongs to a unique duration-class. In order to identify the class of a station s , we define N_c subsets $n(d)$, each of them containing the indexes of the $L_d = |n(d)|$ stations within $n(d)$, with $L_d \leq N, \forall d$ and $\sum_{d=1}^{N_c} L_d = N$. As an example, $n(3) = \{1, 5, 8\}$ means that stations 1, 5, and 8 belong to the third duration-class identified by $d = 3$, and $L_d = 3$.

A. Bi-dimensional Contention Markov Model

The modified bi-dimensional Markov model describing the contention process of the s -th station² in the network is shown in Fig. 1.

Let us elaborate. We consider an overall number of r different backoff stages, starting from the zero-th stage. The maximum Contention Window (CW) size is $W_{max} = 2^m W_0^{(s)}$, with $m \leq r$, whereas the notation $W_i = \min(2^m W_0^{(s)}, 2^i W_0^{(s)})$ is used to identify the i -th contention window size ($W_0^{(s)}$ is the minimum contention window size of the s -th station). Notice that after the m -th stage, the contention window size is fixed to W_{max} for the remaining $(r - m)$ stages, after which the packet is dropped. An additional backoff stage, identified by $(P, -)$, with the same window size of the zero-th stage, is considered on top of the chain in order to account for the post-backoff stage entered by the station after a successful packet transmission, or packet drop [1]. Moreover, the state labelled $(P, 0)$ in Fig. 1, is used for emulating unloaded traffic conditions.

After the post-backoff stage, a station starts a new transmission because a new packet is available in the queue, provided that the channel is sensed idle for DIFS seconds. On the other hand, a new zero-th stage backoff is employed if the channel is sensed busy. Notice that the post-backoff stage is entered only if the station has no longer packets to transmit after a packet transmission; otherwise, a zero-th stage is started. Moreover, if a new packet arrives during a post-backoff stage, the station moves into the zero-th stage, as depicted in Fig. 1. Indeed, backoff stages from 0 to r assume that the station's queue contains at least a packet waiting for transmission.

A packet transmission is attempted only in the states labelled $(i, 0), \forall i = 0, \dots, r$, as well as in the state $(P, 0)$ only if there is a packet in the queue and the channel is sensed idle for DIFS seconds. In case of collision, or due to the fact that transmission is unsuccessful because of channel errors, the backoff stage is incremented and the station moves in the state $(i + 1, k)$, where $k = 0, \dots, W_{i+1} - 1$, with uniform probability P_{eq}/W_{i+1} , whereby P_{eq} , i.e., the probability of equivalent failed transmission, is defined as $P_{eq} = 1 - (1 - P_e)(1 - P_{col}) = P_{col} + P_e - P_e \cdot P_{col}$. Probabilities P_{col} and P_e are, respectively, the collision and the packet error probabilities related to the s -th station.

The transition probabilities for the generic s -th station's Markov process in Fig. 1 could be separated as summarized in what follows, depending on whether transitions start from standard backoff states or from post-backoff states.

Backoff state transitions

$$\begin{aligned}
 P_{i,k|i,k+1} &= 1, & k \in [0, W_i^{(s)} - 2], & i \in [0, r] \\
 P_{P,k|i,0} &= \frac{(1-P_{eq})(1-q)}{W_0^{(s)}}, & k \in [0, W_0^{(s)} - 1], & i \in [0, r - 1] \\
 P_{0,k|i,0} &= \frac{(1-P_{eq})q}{W_0^{(s)}}, & k \in [0, W_0^{(s)} - 1], & i \in [0, r - 1] \\
 P_{P,k|r,0} &= \frac{(1-q)}{W_0^{(s)}}, & k \in [0, W_0^{(s)} - 1], & \\
 P_{0,k|r,0} &= \frac{q}{W_0^{(s)}}, & k \in [0, W_0^{(s)} - 1]. &
 \end{aligned} \tag{1}$$

The meaning of the underlined probabilities is as follows. The first equation in (1) states that, at the beginning of each slot time, the backoff time is decremented. The second (third) equation accounts for the fact that after a successful transmission, the station goes in post-backoff because of an empty (non empty) queue. In both equations, q is used to identify the probability

²In order to keep the notation concise, we omit the apex s over the probabilities involved in the model.

$$\begin{aligned}
\tau_s &= q^2(1 - P_{eq}^{r+1})W_0 \cdot b_{P,0} \\
b_{P,0} &= \left\{ \frac{W_0(W_0+1)}{2}(X_B + X_P) - \left(\frac{qW_0 - (1-q)[1 - (1-q)W_0]}{q^2} \right) X_P + qW_0 \frac{qP_{eq}K + (1-q)}{[1 - (1-q)W_0](1-q)} \right\}^{-1} \\
K &= \frac{1}{2} \left[2W_0 \frac{1 - (2P_{eq})^{m-1}}{1 - 2P_{eq}} + \frac{1 - P_{eq}^{m-1}}{1 - P_{eq}} \right] + (W_m + 1)P_{eq}^{m-1} \frac{1 - P_{eq}^{r-m+1}}{1 - P_{eq}} \\
X_B &= q \frac{W_0 q^2 + (1 - P_i)[1 - (1-q)W_0](1-q)}{W_0[1 - (1-q)W_0](1-q)} \\
X_P &= \frac{q^2}{1 - (1-q)W_0}
\end{aligned} \tag{3}$$

that the queue contains at least a packet waiting for transmission after a time slot, and it will be better defined in Section II-D, where the employed traffic model is described. The fourth equation deals with the situation in which the station has reached the retry limit and, after a packet transmission, the buffer of the station is empty. In this situation, the station moves in the post-backoff stage with an empty queue. The last equation accounts for a scenario similar to the previous one with the difference that, after the packet transmission, the queue is not empty.

Post-backoff state transitions

$$\begin{aligned}
P_{P,k|P,k+1} &= (1 - q) & k \in [0, W_0^{(s)} - 2] \\
P_{0,k|P,k+1} &= q & k \in [0, W_0^{(s)} - 2] \\
P_{P,0|P,0} &= (1 - q) \\
P_{P,k|P,0} &= \frac{qP_i(1 - P_{eq})(1 - q)}{W_0^{(s)}} & k \in [0, W_0^{(s)} - 1] \\
P_{0,k|P,0} &= q \frac{(1 - P_i) + qP_i(1 - P_{eq})}{W_0^{(s)}} & k \in [1, W_0^{(s)} - 1] \\
P_{1,k|P,0} &= \frac{qP_iP_{eq}}{W_1^{(s)}} & k \in [1, W_1^{(s)} - 1]
\end{aligned} \tag{2}$$

The meaning of the underlined probabilities is as follows. The first equation states that the station remains in the post-backoff stage because the queue is empty, whereas the second equation accounts for a transition in the zero-th backoff stage because a new packet arrives at the end of a backoff slot. The third equation models the situation in which there are no packets waiting for transmission, and the station remains in the state $(P, 0)$ (idle state).

The fourth equation deals with the situation in which the station is in the idle state $(P, 0)$, and, at the end of a backoff slot, a new packet arrives in the queue. In this scenario, the packet is successfully transmitted, the queue is empty, and the station moves in another post-backoff stage. The term P_i identifies the probability that the channel is idle, and it is defined as follows with respect to the s -th tagged station:

$$P_i^{(s)} = \prod_{j=1, j \neq s}^N (1 - \tau_j)$$

The fifth equation accounts for a scenario similar to the previous one, except that the station queue is not empty after the immediate transmission of a packet or a situation of busy channel. The last equation models the scenario in which the station goes from the idle state $(P, 0)$ to the first backoff stage because of a failure of the immediate transmission of the packet arrived in the head of the queue.

B. Throughput Evaluation

Next line of pursuit consists in finding the probability τ_s that the s -th station starts a transmission in a randomly chosen time slot. Due to the lengthy algebra involved in the derivations needed for solving the bidimensional Markov chain, the relation that defines τ_s has been derived in an additional document available at [40], whereas for conciseness we show the final formula in (3) (shown at the bottom of this page), along with the other key probabilities needed in this paper. Given τ_s in (3), we can

evaluate the aggregate throughput S as follows:

$$S = \sum_{s=1}^N S_s = \sum_{s=1}^N \frac{1}{T_{av}} P_s^{(s)} \cdot (1 - P_e^{(s)}) \cdot PL^{(s)} \quad (4)$$

whereby T_{av} is the expected time per slot, $PL^{(s)}$ is the packet size of the s -th station, and $P_s^{(s)}$ is the probability of successful packet transmission of the s -th station:

$$P_s^{(s)} = \tau_s \cdot \prod_{\substack{j=1 \\ j \neq s}}^N (1 - \tau_j) \quad (5)$$

The evaluation of the aggregate throughput in (4) requires the knowledge of the expected time per slot, T_{av} . Its evaluation is the focus of the next section.

C. Evaluation of the Expected Time per Slot

The expected time per slot, T_{av} , can be evaluated by weighting the times spent by a station in a particular state with the probability of being in that state. First of all, we observe that there are four different kinds of time slots, with four different average durations:

- the idle slot, in which no station is transmitting over the channel, with average duration T_I ;
- the collision slot, in which more than one station is attempting to gain access to the channel, with average duration T_C ;
- the slot due to erroneous transmissions because of imperfect channel conditions, with average duration T_E ;
- the successful transmission slot, with average duration T_S .

The expected time per slot, T_{av} , can be evaluated by adding the four expected slot durations:

$$T_{av} = T_I + T_C + T_S + T_E. \quad (6)$$

We will now evaluate T_I , T_C , T_S , and T_E .

Upon identifying with σ an idle slot duration, and defining with P_{TR} the probability that the channel is busy in a slot because at least one station is transmitting:

$$P_{TR} = 1 - \prod_{s=1}^N (1 - \tau_s) \quad (7)$$

the average idle slot duration can be evaluated as follows:

$$T_I = (1 - P_{TR}) \cdot \sigma \quad (8)$$

The average slot duration of a successful transmission, T_S , can be found upon averaging the probability $P_s^{(s)}$ that only the s -th tagged station is successfully transmitting over the channel, times the duration $T_S^{(s)}$ of a successful transmission from the s -th station:

$$T_S = \sum_{s=1}^N P_s^{(s)} (1 - P_e^{(s)}) \cdot T_S^{(s)} \quad (9)$$

Notice that the term $(1 - P_e^{(s)})$ accounts for the probability of packet transmission without channel induced errors.

Analogously, the average duration of the slot due to erroneous transmissions can be evaluated as follows:

$$T_E = \sum_{s=1}^N P_s^{(s)} \cdot P_e^{(s)} \cdot T_E^{(s)} \quad (10)$$

Let us focus on the evaluation of the expected collision slot, T_C . There are N_C different values of the collision probability $P_C^{(d)}$, depending on the class of the tagged station identified by d . We assume that in a collision of duration $T_C^{(d)}$ (class- d

collisions), only the stations belonging to the same class, or to higher classes (i.e., stations whose channel occupancy is lower than the one of stations belonging to the tagged station indexed by d) might be involved.

In order to identify the collision probability $P_C^{(d)}$, let us first define the following three transmission probabilities ($P_{TR}^{C(d)}$, $P_{TR}^{H(d)}$, $P_{TR}^{L(d)}$) under the hypothesis that the tagged station belongs to the class d . Probability $P_{TR}^{L(d)}$ represents the probability that at least another station belonging to a lower class transmits, and it can be evaluated as

$$P_{TR}^{L(d)} = 1 - \prod_{i=1}^{d-1} \prod_{s \in n(i)} (1 - \tau_s) \quad (11)$$

Probability $P_{TR}^{H(d)}$ is the probability that at least one station belonging to a higher class transmits, and it can be evaluated as

$$P_{TR}^{H(d)} = 1 - \prod_{i=d+1}^{N_c} \prod_{s \in n(i)} (1 - \tau_s) \quad (12)$$

Probability $P_{TR}^{C(d)}$ represents the probability that at least a station in the same class d transmits:

$$P_{TR}^{C(d)} = 1 - \prod_{s \in n(d)} (1 - \tau_s) \quad (13)$$

Therefore, the collision probability for a generic class d takes into account only collisions between at least one station of class d and at least one station within the same class (internal collisions) or belonging to higher class (external collisions). Hence, the total collision probability can be evaluated as:

$$P_C^{(d)} = P_C^{I(d)} + P_C^{E(d)} \quad (14)$$

whereby

$$P_C^{I(d)} = (1 - P_{TR}^{H(d)}) \cdot (1 - P_{TR}^{L(d)}) \cdot \left[P_{TR}^{C(d)} - \sum_{s \in n(d)} \tau_s \prod_{j \in n(d), j \neq s} (1 - \tau_j) \right] \quad (15)$$

represents the internal collisions between at least two stations within the same class d , while the remaining are silent, and

$$P_C^{E(d)} = P_{TR}^{C(d)} \cdot P_{TR}^{H(d)} \cdot (1 - P_{TR}^{L(d)}) \quad (16)$$

concerns to the external collisions with at least one station of class higher than d .

Finally, the expected duration of a collision slot is:

$$T_C = \sum_{d=1}^{N_c} P_C^{(d)} \cdot T_C^{(d)} \quad (17)$$

Constant time durations $T_S^{(s)}$, $T_E^{(s)}$ and $T_C^{(d)}$ are defined in a manner similar to [22] with the slight difference that the first two durations are associated to a generic station s , while the latter is associated to each duration class, which depends on the combination of both payload length and data rate of the station of class d .

D. Traffic Model

The employed traffic model for each station assumes a Poisson distributed packet arrival process, whereby the inter-arrival times among packets are exponentially distributed with mean $1/\lambda_t$. In order to greatly simplify the analysis, we consider small queue, as proposed in [12], even though the proposed analysis may be easily extended to queues with any length. The traffic of each station is accounted for within the Markov model by employing a probability³, q , that accounts for the scenario whereby

³A superscript (t) is used for discerning the probability q among the stations.

at least one packet is available in the queue at the end of a slot. In our setting, each station is characterized by its own traffic, and the probability $q^{(t)}$ of the t -th station can be evaluated by averaging over the four types of time slots, namely idle, success, collision, and channel error time slot. Upon noticing that, with the underlined packet model, the probability of having at least one packet arrival during time T is equal to $1 - e^{-\lambda_t \cdot T}$, $q^{(t)}$ can be evaluated as:

$$\begin{aligned}
q^{(t)} &= (1 - P_{TR}) \cdot (1 - e^{-\lambda_t \cdot \sigma}) + \\
&+ \sum_{s=1}^N P_s^{(s)} \left(1 - P_e^{(s)}\right) \cdot (1 - e^{-\lambda_t \cdot T_s^{(s)}}) + \\
&+ \sum_{s=1}^N P_s^{(s)} \cdot P_e^{(s)} \cdot (1 - e^{-\lambda_t \cdot T_E^{(s)}}) + \\
&+ \sum_{d=1}^{N_c} P_C^{(d)} \cdot (1 - e^{-\lambda_t \cdot T_C^{(d)}})
\end{aligned} \tag{18}$$

whereby the probabilities P_{TR} , $P_s^{(s)}$, and $P_C^{(d)}$ are, respectively, as defined in (7), (5), and (14), whereas $P_e^{(s)}$ is the packet error rate of the s -th station.

III. EVALUATING THE NETWORK LOADING CONDITIONS

In a previous paper [14], we proved that the behaviour of the aggregate throughput in a network of N homogeneous⁴ contending stations is a linear function of the packet arrival rate λ with a slope depending on both the number of contending stations and the average payload length. We also derived the interval of validity of the proposed model by showing the presence of a critical λ , above which all the stations begin operating in saturated traffic conditions.

This kind of behaviour, with appropriate generalizations, is also observed when multirate and variable loaded stations are present in the network. We have to identify a set of conditions for a network to be considered as loaded. We notice in passing that this framework is not generally considered in the literature, since most papers assume saturated traffic conditions. A key observation from the analysis developed in this section is that in an unloaded network there is no need to guarantee fairness, since each contending stations can transmit its packets at its own pace, regardless of its minimum CW, as well as other network parameters.

Under the traffic model described in section II-D, we define unloaded a network in which each contending station has a packet rate λ_t less than or equal to its packet service rate $\tilde{\mu}_S^{(t)}$:

$$\lambda_t \leq \tilde{\mu}_S^{(t)}, \quad \forall t \in \{1, \dots, N\} \tag{19}$$

The reason is simple: this condition ensures that the average packet inter-arrival time is greater than or equal to the average service time of the t -th station. In such a scenario, the probabilities of collisions among stations are very low, and each contending station is able, on the average, to gain the access to the channel as soon as a new packet arrives in its queue. Notice that $\tilde{\mu}_S^{(t)}$ only depends on the packet rates λ_i of the other $N - 1$ stations other than the tagged one.

The evaluation of the packet service rate $\tilde{\mu}_S^{(t)}$ in a multirate and heterogeneous network is quite difficult [12] since packet arrivals may occur during the stage of post-backoff, as well as during the usual backoff stages accomplished by each station before gaining the channel for transmission. Since we are interested in a threshold which differentiates the unsaturated from the saturated loading conditions of the stations, we can employ an upper bound defined by the *saturation* service rate, identified as $\mu_S^{(t)}$, in place of the actual service rate $\tilde{\mu}_S^{(t)}$. The advantage relies on the observation that such a bound is always evaluated considering a post-backoff stage. Indeed, after a packet transmission, a new packet is always available in the queue assuming saturated traffic; therefore, the service time starts from a post-backoff phase whereby the contention window is $W_0^{(s)}$. We

⁴By homogeneous we simply mean that the network is characterized by N stations transmitting with the same bit rate (no multirate hypothesis) and the same load.

notice that the saturation service time always includes the post-backoff stage, thus its duration is longer than the actual service time evaluated without considering the post-backoff time.

Hence, in the remaining part of this section, we evaluate the saturation service rate $\mu_S^{(t)} = 1/T_{serv}^{(t)}$, i.e., the rate at which packets are taken from the queue of the t -th station under saturated conditions.

Upon considering the tagged station identified by the index $t \in \{1, \dots, N\}$, the saturation service time $T_{serv}^{(t)}$ can be defined as follows [28]:

$$T_{serv}^{(t)} = \left\{ \sum_{i=0}^r (P_{eq}^{(t)})^i \left(iT_C + \sum_{j=0}^i \overline{W}_j^{(t)} \cdot T_{bo}^{(t)} + T_S^{(t)} \right) + \underbrace{(P_{eq}^{(t)})^{r+1} \left((r+1)T_C + \sum_{j=0}^r \overline{W}_j^{(t)} \cdot T_{bo}^{(t)} \right)}_{DRO P} \right\} / \sum_{j=0}^{r+1} (P_{eq}^{(t)})^j \quad (20)$$

The first term in the summation represents the average time that a station spends through the backoff stages from 0 to r before transmitting a packet, i.e., the so called MAC access time. We notice that for the i -th stage, i collisions of average duration T_C , as well as i backoff stages from 0 to i (each of them with an average number $\overline{W}_j^{(t)}$ of slot of duration $T_{bo}^{(t)}$) occurred, after which the packet is successfully transmitted with duration $T_S^{(t)}$. The second term of the summation takes into account the average duration of a packet drop that occurs after $(r+1)$ collisions and backoff stages. The whole summation is scaled by a normalization factor that takes into account the probability set over which the service time is evaluated.

The average number of slots for the i backoff stages, is defined as

$$\overline{W}_j^{(t)} = (2^{\min(j,m)} \cdot W_0^{(t)} - 1)/2.$$

Each slot has average duration $T_{bo}^{(t)}$, which is substantially evaluated as T_{av} in (6) except that the tagged station (t) is not considered because it is either idle, or in a backoff state.

Let us discuss two sample scenarios in order to derive a variety of observations that are at the very basis of the fairness problem developed in the next section. The network parameters used in the investigated IEEE802.11b MAC layer are reported in Table I [1]. The first investigated scenario considers a network of 3 contending stations. Two stations, namely S2 and S3, transmit packets with constant rates $\lambda = 100$ pkt/s and $\lambda = 500$ pkt/s, respectively. The bit rate of the two stations S2 and S3 is 11 Mbps. The third station, S1, has a bit rate equal to 1 Mbps and a packet rate λ_1 that is varied in the range $[0, 2000]$ pkt/s in order to investigate its effects on the network load. The behaviour of the three ratios $\lambda_t/\mu_S^{(t)}$ is shown in Fig. 2. Some observations are in order. First of all, notice that as far as S1 increases its packet rate, the curves $\lambda_2 \cdot T_{serv}^{(2)}$ and $\lambda_3 \cdot T_{serv}^{(3)}$ tend to increase because of the increasing values of the service times $T_{serv}^{(2)}$ and $T_{serv}^{(3)}$ experienced by S2 and S3. Notice that, as λ_1 increases, the slowest station S1 tends to transmit more often. The station S3 goes in loaded condition when $\lambda_1 \approx 20$ pkt/s, while S2 can be considered loaded for $\lambda_1 \approx 200$ pkt/s. When a station becomes loaded, the incoming packets tend to be stored in the station queue waiting for transmission since the service rate, i.e., the number of packets that on average are serviced by the MAC, is below the rate by which the packets arrive in the station queue.

The per-station throughput achieved by the three stations in the investigated scenario is shown in Fig. 3. The throughput gained by the two fastest stations, S2 and S3, tends to decrease because of the anomaly problem in the multirate scenario: the slowest station tends to occupy the channel longer and longer as far as its packet rate λ_1 increases. In the same figure, we show two tick curves. The horizontal line L2 corresponds to the saturation throughput of S1, while the straight line L1 is the tangent to the throughput curve passing through the origin. For very small values of λ_1 , the throughput of the station S1 grows linearly with λ_1 . Packets are mainly transmitted as soon as they arrive at the MAC layer, and the station throughput is

approximately equal to $\lambda_1 \cdot PL^{(1)}$. However, when the station approaches the transition point $\lambda_1^* = 89.19$ pkt/s derived with the proposed framework (this is the value of λ_1 corresponding to the relation $\lambda_1/\mu_S^{(1)} = 1$), the throughput curve tends to reach the asymptote L2, which corresponds to the saturation throughput of S1. Notice that the curve L2 approximately corresponds to 0.73 Mbps, which is $\lambda_1^* \cdot PL^{(1)} = 89.19 \cdot 1028 \cdot 8$ bps.

In the second scenario, the stations S1 and S2 are interested by a constant packet rate noticed in the label of Fig. 4. These two stations do not get loaded by the increasing packet rate of the station S3 since the curves $\lambda_1/\mu_S^{(1)}$ and $\lambda_2/\mu_S^{(2)}$ are strictly less than one. As a consequence, the per-station throughput of both S1 and S2 is approximately constant across the range of values of the packet rate λ_3 as noticed in Fig. 5. On the other hand, the throughput achieved by the station S3 tends to saturate as soon as λ_3 reaches the value 533 pkt/s noticed in Fig. 4.

In the light of the previous two sample scenario, let us summarize the main ingredients of the results proposed in this section. As observed in the two previous sample scenarios, this method allows to identify whether the network is loaded by establishing the thresholds of each contending station in the network. This issue has been overlooked in the literature, where the saturation assumption is widely adopted. Moreover, this issue is at the very basis of any throughput optimization strategy since an unloaded network does not need to be optimized.

We say that the network is loaded when every station has a traffic above its proper threshold. On the other hand, it should be noticed that a network can be unloaded even if a subset of the stations is loaded. This was the case of the second scenario described above, where, despite the fact that the station S3 was interested by an increasing traffic load λ_3 , the stations S1 and S2 did not experience any performance loss (see Fig. 5) because their traffics were below the respective thresholds.

IV. THE PROPORTIONAL FAIRNESS THROUGHPUT ALLOCATION ALGORITHM

This section presents the novel throughput allocation criterion, which aims at improving fairness among the N contending stations. In order to face the fairness problem in the most general scenario, i.e., multirate DCF and general station loading conditions, we propose a novel Proportional Fairness Criterion (PFC) by starting from the PCF defined by Kelly in [41], and employed in [25] in connection to proportional fairness throughput allocation in multirate and saturated DCF operations.

It is known that one of the main drawbacks of the basic DCF operating in a multirate scenario relies on the fact that it behaves in such a way as to guarantee equal long-term channel access probability to the various contending stations [25], [30]. In order to solve this problem, various optimization algorithms have been proposed in the literature (see, for instance, [25]-[37]). These contributions allowed to highlight the behaviour of the DCF as well as various drawbacks when operating in a multirate scenario. For instance, it is known that the aggregate throughput of multirate IEEE802.11-like networks is optimized when only the high rate stations transmit, while the low rate stations are kept silent. Of course, this result is not desirable from a fairness point of view, even though it mitigates the DCF performance anomaly noticed in [2].

To the best of our knowledge, the solutions proposed so far in the literature refer to homogeneous networks in that all the contending stations operate with the same traffic, as exemplified by the station packet rate λ_s , and channel conditions. Furthermore, almost all the works focus on saturated traffic conditions. As already mentioned before, in a practical setting the contending stations have their own traffic and are affected by different channel conditions. The key observation here is that a fair throughput allocation should account for the station packet rate, as well as for the specific channel conditions experienced by each contending station.

Let us briefly mention the rationales at the very basis of the PFC. A proportional fairness optimization criterion allocates to each station a throughput *proportional* to the station transmission rate. Resorting to the notation proposed in [41], a throughput

allocation vector $\underline{x} = \{x_s; s = 1, \dots, N\}$ is *proportional fair* if the following condition holds:

$$\sum_{s=1}^N \frac{y_s^* - x_s}{x_s} \leq 0 \quad (21)$$

for any other feasible throughput allocation vector \underline{y}^* . The PFC maximization problem, which satisfies (21), can be formalized as follows:

$$\begin{aligned} \max \quad & \sum_{s=1}^N \log(x_s) \\ \text{over} \quad & x_s \in [0, x_{s,m}], \quad s = 1, \dots, N \end{aligned} \quad (22)$$

whereby $x_{s,m}$ is the maximum throughput of the s -th station. Due to the strict concavity of the logarithmic function and because of the compactness of the feasible region $x_s \in [0, x_{s,m}]$, $s = 1, \dots, N$, there exists a unique solution to the optimization problem (22). This implies that a local maximum is also global.

Given these preliminaries, in the proposed model, the traffic of each station is characterized by the packet arrival rate λ_s , which depends mainly on the application layer. Let λ_{max} be the maximum packet rate among $\lambda_1, \dots, \lambda_N$.

Consider the following modified optimization problem:

$$\begin{aligned} \max \quad & U = U(S_1, \dots, S_N) = \sum_{s=1}^N \frac{\lambda_s}{\lambda_{max}} \cdot \log(S_s) \\ \text{subject to} \quad & S_s \in [0, S_{s,m}], \quad s = 1, \dots, N \end{aligned} \quad (23)$$

whereby S_s is the throughput of the s -th station, and $S_{s,m}$ is its maximum value, which equals the station bit rate $R_d^{(s)}$. In our scenario, the individual throughputs, S_s , are interlaced because of the interdependence of the probabilities involved in the transmission probabilities $\tau_s, \forall s = 1, \dots, N$. For this reason, we reformulate the maximization problem in order to find the N optimal values of τ_s for which the cost function U in (23) gets maximized. The optimal values τ_s^* are then used to set the network parameters of each station.

Due to the compactness of the feasible region $S_s \in [0, S_{s,m}], \forall s$, the maximum of $U(S_1, \dots, S_N)$ can be found among the solutions of $\nabla U = \left(\frac{\partial U}{\partial \tau_1}, \dots, \frac{\partial U}{\partial \tau_N} \right) = 0$. After some algebra (the derivations are reported in the Appendix), the solutions can be written as:

$$\frac{\lambda_j}{\lambda_{max}} \frac{1}{\tau_j} - \frac{1}{1 - \tau_j} \sum_{k=1, k \neq j}^N \frac{\lambda_k}{\lambda_{max}} = \frac{C}{T_{av}} \frac{\partial T_{av}}{\partial \tau_j}, \quad \forall j = 1, \dots, N \quad (24)$$

whereby $C = \sum_{i=1}^N \frac{\lambda_i}{\lambda_{max}}$, and T_{av} is a function of τ_1, \dots, τ_N as noticed in (6).

Due to the presence of T_{av} , a closed form of the maximum of $U(S_1, \dots, S_N)$ cannot be found. Notice that it is quite difficult to derive the contribution of the partial derivative of T_{av} on τ_j , especially when $N \gg 1$, because of the huge number of network parameters belonging to different stations. The definition of T_{av} in (6) is composed by four different terms, which include the whole set of $\tau_s, \forall s$. In order to overcome this problem, we first numerically obtain the optimal values $\tau_s^*, \forall s$ from (24), then, we choose the value of the minimum contention window size, $W_0^{(s)}$, by equating the optimizing τ_s^* to (3) for any s .

The optimization criterion summarized in (23) will be denoted as Load Proportional Fairness (LPF) criterion in the following.

Let us derive some observations on the proposed throughput allocation algorithm by contrasting it to the classical PF algorithm. Consider two contending stations with packet rates $\lambda_1 = 50$ pkt/s and $\lambda_2 = 100$ pkt/s, respectively. Employing the classical PF method, a throughput allocation is proportionally fair if a reduction of $x\%$ of the throughput allocated to one station is counterbalanced by an increase of more than $x\%$ of the throughputs allocated to the other contending stations.

In our setup, the ratio λ_1/λ_2 can be interpreted as the frequency by which the first station tries to get access to the channel relative to the other station. Therefore, a throughput allocation is proportionally fair if, for instance, a reduction of 20% of the throughput allocated to the first station, which has a relative frequency of 1/2, is counterbalanced by an increase of more than 40% of the throughput allocated to the second station. In a scenario with multiple contending stations, the relative frequency is evaluated with respect to the station with the highest packet rate in the network, that gets unitary relative frequency.

Based on extensive analysis, we found that the optimization problem (23) sometimes yields throughput allocations that cannot be actually managed by the stations. As a reference example, assume that, due to the specific channel conditions experienced, the first station has a bit rate equal to 1 Mbps and needs to transmits 200 pkt/s. Given a packet size of 1024 bytes, that is 8192 bits, the first station would need to transmit $8192 \times 200 \text{ bps} \approx 1.64\text{Mbps}$ far above the maximum bit rate decided at the physical layer. In this scenario, such a station could not send over the channel a throughput greater than 1Mbps. The same applies to the other contending stations in the network experiencing similar conditions. In order to face this issue, we considered the following optimization problem

$$\begin{aligned} \max \quad & \sum_{s=1}^N \frac{\lambda_s^*}{\lambda_{max}^*} \cdot \log(S_s) \\ \text{over} \quad & S_s \in [0, S_{s,m}], \quad s = 1, \dots, N \end{aligned} \quad (25)$$

where $\forall s = 1, \dots, N$,

$$\lambda_s^* = \begin{cases} \lambda_s, & \text{if } \lambda_s \cdot PL^{(s)} \cdot 8 \leq R_d^{(s)} \\ \frac{R_d^{(s)}}{8 \cdot PL^{(s)}}, & \text{if } \lambda_s \cdot PL^{(s)} \cdot 8 > R_d^{(s)} \end{cases}$$

and $\lambda_{max}^* = \max_s \lambda_s^*$. The allocation problem in (25), solved as for the LPF in (23), guarantees a throughput allocation which is proportional to the frequency of channel access of each station relative to their actual ability in managing such traffic. The idea relies on the observation that it is not optimal to allocate a throughput that the station cannot actually manage.

The optimization criterion summarized in (25) will be denoted as Modified Load Proportional Fairness (MLPF) criterion in what follows. As in the case of the LPF criterion, the MLPF optimization problem in (25) is solved by first numerically obtaining the optimal values $\tau_s^*, \forall s$, and then choosing the value of the minimum contention window sizes $W_0^{(s)}$ by equating the optimizing τ_s^* to (3) independently for any s .

V. SIMULATION RESULTS

This section presents simulation results obtained for a variety of network scenarios optimized with the fairness criteria proposed in the previous section.

We have developed a C++ simulator modelling both the DCF protocol details in 802.11b and the backoff procedures of a specific number of independent transmitting stations. The simulator considers an Infrastructure BSS (Basic Service Set) with an Access Point (AP) and a certain number of fix stations which communicate only with the AP. Traffic is generated following the exponential distribution for the packet interarrival times. Moreover, the MAC layer is managed by a state machine which follows the main directives specified in the standard [1], namely waiting times (DIFS, SIFS, EIFS), post-backoff, backoff, basic and RTS/CTS access modes. The typical MAC layer parameters for IEEE802.11b reported in Table I [1] have been used for performance validation.

The first investigated scenario, namely scenario A, considers a network with 3 contending stations. Two stations transmit packets with rate $\lambda = 500 \text{ pkt/s}$ at 11 Mbps. The payload size, assumed to be common to all the stations, is $PL = 1028$ bytes. The third station has a bit rate equal to 1Mbps and a packet rate $\lambda = 1000 \text{ pkt/s}$.

From (19), it is straightforward to notice that the scenario A refers to a loaded network. Fig. 6 shows the service rates $\mu_S^{(t)}$ of the three contending stations as a function of the packet rate λ_1 of the station transmitting at 1 Mbps. The operating point of the considered scenario A is highlighted in Fig. 6. Notice that, since the service rates $\mu_S^{(t)}$ of the three stations are below the respective packet rates λ_t , the network is loaded. Moreover, the service rates of the three stations tend to the same values because of the rate anomaly problem: the station transmitting at 1 Mbps reduces the service rates of the other stations.

The simulated normalized throughput achieved by each station in this scenario is depicted in the left subplot of Fig. 7 for the following four setups. The three bars labelled 1-DCF represent the normalized throughput achieved by the three stations with a classical DCF. The second set of bars, labelled 2-PF, identifies the simulated normalized throughput achieved by the DCF optimized with the PF criterion [25], [41], whereby the actual packet rates of the stations are not considered. The third set of bars, labelled 3-LPF, represents the normalized throughput achieved by the three stations when the allocation problem (23) is employed. Finally, the last set of bars, labelled 4-MLPF, represents the simulated normalized throughput achieved by the contending stations when the CW sizes are optimized with the modified fairness criterion in (25). Notice that the throughput allocations guaranteed by LPF and MLPF improve over the classical DCF. When the station packet rate is considered in the optimization framework, a higher throughput is allocated to the first station presenting the maximum value of λ among the considered stations. However, the highest aggregate throughput is achieved when the allocation is accomplished with the optimization framework 4-MLPF. The reason for this behaviour is related to the fact that the first station requires a traffic equal to $8.22 \text{ Mbps} = 10^3 \text{ pkt/s} \cdot 1028 \text{ bytes/pkt} \cdot 8 \text{ bits/pkt}$, which is far above the maximum traffic (1 Mbps) that the station would be able to deal with in the best scenario. In this respect, the MLPF criterion results in better throughput allocations since it accounts for the real traffic that the contending station would be able to deal with in the specific scenario at hand.

Similar considerations can be drawn from the results shown in the right subplot of Fig. 7 (related to scenario B), whereby in the simulated scenario the two fastest stations are also characterized by a packet rate greater than the one of the slowest station. Notice that the optimization framework 3-LPF is able to guarantee improved aggregate throughput with respect to both the non-optimized DCF and the classical PF algorithms. The operating point of the scenario B is highlighted in Fig. 6; based on the considerations above, this is a loaded network as well.

The aggregate throughputs achieved in the two investigated scenarios are as follows:

Scenarios		1-DCF	2-PF	3-LPF	4-MLPF
A	Jain's Index	0.451	0.872	0.724	0.848
	S [Mbps]	1.85	3.60	3.10	5.07
B	Jain's Index	0.474	0.881	0.976	0.847
	S [Mbps]	1.99	3.63	4.62	5.07

whereby we also show the fairness Jain's index [42] evaluated on the normalized throughputs noted in the subplots of Fig. 7. It is worth noticing that the proposed MLPF throughput allocation criterion is able to guarantee improved aggregate throughput relative to both the classical DCF and the PF algorithm, with fairness levels on the same order of the ones guaranteed by the classical PF algorithm.

For the sake of investigating the behaviour of the proposed allocation criteria as a function of the packet rate of the slowest station, we simulated the throughput allocated to a network composed by three stations, whereby the slowest station, transmitting

at 1Mbps, presents an increasing packet rate in the range 10–3000 pkt/s. The other two stations transmit packets at the constant rate $\lambda = 500$ pkt/s at 11 Mbps. The simulated throughput of the three contending stations is shown in the three subplot of Fig. 8 for the unoptimized DCF, as well as for the two criteria LPF and MLPF. Some considerations are in order. Let us focus on the throughput of the DCF (uppermost subplot in Fig. 8). As far as the packet rate of the slowest station increases, the throughput allocated to the fastest stations decreases quite fast because of the performance anomaly of the DCF [2]. The three stations reach the same throughput when the slowest station presents a packet rate equal to 500 pkt/s, corresponding to the one of the other two stations. From $\lambda = 500$ pkt/s all the way up to 3000 pkt/s, the throughput of the three stations do not change anymore, since all the stations have a throughput imposed by the slowest station in the network. Let us focus on the results shown in the other two subplots of Fig. 8, labelled LPF and MLPF, respectively. A quick comparison among these three subplots in Fig. 8 reveals that the MLPF allocation criterion guarantees improved aggregate throughput for a wide range of packet rates of the slowest station, greatly mitigating the rate anomaly problem of the classical DCF operating in a multirate setting. In terms of aggregate throughput, the best solution is achieved with the MLPF criterion, which avoids that the slowest station receives a throughput allocation that would not be able to employ due to its reduced bit rate (1 Mbps).

VI. CONCLUSIONS

Focusing on multirate IEEE 802.11 Wireless LAN employing the mandatory Distributed Coordination Function (DCF) option, this paper established the conditions under which a network constituted by a certain number of stations transmitting with their own bit rates and packet rates can be considered loaded. It then proposed a modified proportional fairness criterion suitable for mitigating the *rate anomaly* problem of multirate loaded IEEE 802.11 Wireless LANs.

Simulation results were presented for some sample scenarios showing that the proposed throughput allocation was able to greatly increase the aggregate throughput of the DCF, while ensuring fairness levels among the stations of the same order of the ones available with the classical proportional fairness criterion.

REFERENCES

- [1] *IEEE Standard for Wireless LAN Medium Access Control (MAC) and Physical Layer (PHY) Specifications*, November 1997, P802.11
- [2] M. Heusse, F. Rousseau, G. Berger-Sabbatel, and A. Duda, "Performance anomaly of 802.11b" *In Proc. of IEEE INFOCOM 2003*, pp. 836-843.
- [3] G. Bianchi, "Performance analysis of the IEEE 802.11 distributed coordination function", *IEEE JSAC*, Vol.18, No.3, March 2000.
- [4] H.C. Lee, "Impact of bit errors on the DCF throughput in wireless LAN over ricean fading channels", *In Proc. of IEEE ICDT '06*, 2006.
- [5] Q. Ni, T. Li, T. Turletti, and Y. Xiao, "Saturation throughput analysis of error-prone 802.11 wireless networks", *Wiley Journal of Wireless Communications and Mobile Computing*, Vol. 5, No. 8, pp. 945-956, Dec. 2005.
- [6] P. Chatzimisios, A.C. Boucouvalas, and V. Vitsas, "Influence of channel BER on IEEE 802.11 DCF", *IEE Electronics Letters*, Vol.39, No.23, pp.1687-1689, Nov. 2003.
- [7] M. Zorzi and R.R. Rao, "Capture and retransmission control in mobile radio", *IEEE JSAC*, Vol.12, No.8, pp.1289 - 1298, Oct. 1994.
- [8] J.H. Kim and J.K. Lee, "Capture effects of wireless CSMA/CA protocols in Rayleigh and shadow fading channels", *IEEE Trans. on Veh. Tech.*, Vol.48, No.4, pp.1277-1286, July 1999.
- [9] Z. Hadzi-Velkov and B. Spasenovski, "Capture effect in IEEE 802.11 basic service area under influence of Rayleigh fading and near/far effect", *In Proc. of 13th IEEE International Symposium on Personal, Indoor and Mobile Radio Communications*, Vol.1, pp.172-176, Sept. 2002.
- [10] F. Daneshgaran, M. Laddomada, F. Mesiti, M. Mondin, and M. Zanolò, "Saturation throughput analysis of IEEE 802.11 in presence of non ideal transmission channel and capture effects," *IEEE Trans. on Communications*, Vol. 56, No. 7, pp.1178-1188, July 2008..
- [11] L.Y. Shyang, A. Dadej, and A.Jayasuriya, "Performance analysis of IEEE 802.11 DCF under limited load", *In Proc. of Asia-Pacific Conference on Communications*, Vol.1, pp.759-763, 03-05 Oct. 2005.
- [12] D. Malone, K. Duffy, and D.J. Leith, "Modeling the 802.11 distributed coordination function in non-saturated heterogeneous conditions", *IEEE-ACM Trans. on Networking*, vol. 15, No. 1, pp. 159172, Feb. 2007.

- [13] F. Daneshgaran, M. Laddomada, F. Mesiti, and M. Mondin, "A model of the IEEE 802.11 DCF in presence of non ideal transmission channel and capture effects," *In Proc. of IEEE Globecom 07*, Washington DC, November 2007.
- [14] F. Daneshgaran, M. Laddomada, F. Mesiti, and M. Mondin, "Unsaturated throughput analysis of IEEE 802.11 in presence of non ideal transmission channel and capture effects," *IEEE Trans. on Wireless Communications*, Vol. 7, No. 4, pp. 1276-1286, April 2008.
- [15] W. Lee, C. Wang, and K. Sohraby, "On use of traditional M/G/1 model for IEEE 802.11 DCF in unsaturated traffic conditions", *In Proc. of IEEE WCNC*, 2006, pp. 1933-1937.
- [16] H. Zhai, Y. Kwon, and Y. Fang, "Performance analysis of IEEE 802.11 MAC protocols in wireless LANs," *Wireless Communications and Mobile Computing*, vol. 4, issue 8, pp. 917-931, Dec. 2004.
- [17] Y. Zheng, K. Lu, D. Wu, and Y. Fang, "Performance analysis of IEEE 802.11 DCF in imperfect channels," *IEEE Transactions on Vehicular Technology*, Vol. 55, No. 5, pp. 1648-1656, Sept. 2006.
- [18] F. Daneshgaran, M. Laddomada, F. Mesiti, and M. Mondin, "On the linear behaviour of the throughput of IEEE 802.11 DCF in non-saturated conditions", *IEEE Communications Letters*, Vol. 11, No. 11, pp. 856-858, Nov. 2007.
- [19] D. Qiao, S. Choi, and K.G. Shin, "Goodput analysis and link adaptation for IEEE 802.11a wireless LANs", *IEEE Trans. On Mobile Computing*, Vol.1, No.4, Oct.-Dec. 2002.
- [20] T. Joshi, A. Mukherjee, and D.P. Agrawal, "Analytical modeling of the link delay characteristics for IEEE 802.11 DCF multi-rate WLANs," *In Proc. of IEEE CCECE-CCGEI*, pp. 2164-2167, May 2006.
- [21] G.R. Cantieni, Q. Ni, C. Barakat, and T. Tuletto, "Performance analysis under finite load and improvements for multirate 802.11," *Computer Communications*, Elsevier, vol.28, No.10, pp.1095-1109, June 2005.
- [22] F. Daneshgaran, M. Laddomada, F. Mesiti, and M. Mondin, "Modelling and analysis of the distributed coordination function of IEEE 802.11 with multirate capability", *In Proc. of IEEE WCNC 2008*, March 2008.
- [23] D.-Y. Yang, T.-J. Lee, K. Jang, J.-B. Chang, and S. Choi, "Performance enhancement of multirate IEEE 802.11 WLANs with geographically scattered stations," *IEEE Trans. on Mobile Computing*, vol.5, no.7, pp.906-919, July 2006.
- [24] M. Ergen and P. Varaiya, "Formulation of distribution coordination function of IEEE 802.11 for asynchronous networks: Mixed data rate and packet size", *IEEE Trans. on Vehicular Technology*, Vol.57, No.1, pp.436-447, Jan. 2008.
- [25] A. Banchs, P. Serrano, and H. Oliver, "Proportional fair throughput allocation in multirate IEEE 802.11e wireless LANs", *Wireless Networks*, Vol 13, No. 5, pages 649-662, May 2007.
- [26] I. Tinnirello and S. Choi, "Temporal fairness provisioning in multi-rate contention-based 802.11e WLANs", *In Proc. of Sixth IEEE Int. Symp. on WoWMoM 2005*, pp.220 - 230, June 2005.
- [27] G. Tan and J. Guttag, "Time-based fairness improves performance in multi-rate WLANs", *USENIX Annual Technical Conference*, June 27-July 2, 2004, Boston, MA, USA.
- [28] A.V. Babu, L. Jacob, and V. Brijith, "A novel scheme for achieving time based fairness in IEEE 802.11 multirate wireless LANs", *In Proc. of 13th IEEE International Conference on Networks 2005*, Vol.1, pp.16-18, November 2005.
- [29] T. Joshi, A. Mukherjee, Y. Yoo, and D. P. Agrawal, "Air time fairness for IEEE 802.11 multi rate networks", *IEEE Trans. on Mobile Computing*, to appear 2008.
- [30] A.V. Babu and L. Jacob, "Fairness analysis of IEEE 802.11 multirate wireless LANs", *IEEE Trans. on Vehicular Technology*, Vol.56, No.5, pp.3073-3088, Sept. 2007.
- [31] L. B. Jiang and S. C. Liew, "Proportional fairness in wireless LANs and ad hoc networks", *In Proc. of IEEE WCNC 2005*, Vol.3, pp.1551-1556, New Orleans, LA, USA, 13-17 March 2005.
- [32] X. Tian, X. Chen, T. Ideguchi, and Y. Fang, "Improving throughput and fairness in WLANs through dynamically optimizing backoff", *IEICE Trans. on Communications*, Vol.E88-B, No.11, pp.4328-4338, November 2005.
- [33] A. Khalaj, N. Yazdani, and M. Rahgozar, "Effect of the contention window size on performance and fairness of the IEEE 802.11 standard", *Wireless Personal Comm.*, Vol. 43, No. 4, pp. 1267-1278, Dec. 2007.
- [34] S. Choudhury and J. D. Gibson, "Throughput optimization for wireless LANs in the presence of packet error rate constraints", *IEEE Communications Letters*, Vol.12, No.1, pp.11-13, January 2008.
- [35] H. Anouar and C. Bonnet, "Optimal constant-window backoff scheme for IEEE 802.11 DCF in single-hop wireless networks under finite load conditions", *Wireless Personal Comm.*, Vol. 43, No. 4, pp. 1583-1602, Dec. 2007.
- [36] Y. Peng, SD Cheng, and JL Chen, "RSAD: A robust distributed contention-based adaptive mechanism for IEEE 802.11 wireless LANs", *Journal of Computer Science and Technology*, Vol. 20, No. 2, pp. 282-288, March 2005.
- [37] Q. Xia and M. Hamdi, "Contention window adjustment for IEEE 802.11 WLANs: A control-theoretic approach", *In Proc. of IEEE ICC 2006*, Vol. 9, pp.3923 - 3928, June 2006.

- [38] F. Cali, M. Conti, and E. Gregori, "Dynamic tuning of the IEEE 802.11 protocol to achieve a theoretical throughput limit", *IEEE/ACM Trans. On Networking*, Vol.8, No.6, pp.785-799, December 2000.
- [39] S. Choudhury and J. D. Gibson, "Payload length and rate adaptation for multimedia communications in wireless LANs", *IEEE JSAC*, Vol.25, No.4, pp.796-807, May 2007.
- [40] http://www.tlc.polito.it/dcc_team/research.php?id=9
- [41] F. Kelly, "Charging and rate control for elastic traffic", *European Trans. on Telecommunications*, Vol.8, No.1, pp.33-37, January 1997.
- [42] R. Jain, D. Chiu, and W. Hawe, "A quantitative measure of fairness and discrimination for resource allocation in shared computer systems", *Digital Equip. Corp., Littleton, MA, DEC Rep., DEC-TR-301, September 1984*.
- [43] G. Bolch, S. Greiner, H. de Meer, and K.S. Trivedi, *Queueing Networks and Markov Chains*, Wiley-Interscience, 2nd edition, 2006.

APPENDIX

The objective of this section is to derive the maximum of the function $U(S_1, \dots, S_N)$ in (23) as a function of $\tau_s, \forall s = 1, \dots, N$.

Upon substituting (5) and (6) in (4), and deriving with respect to τ_j , we obtain:

$$\begin{aligned}
& \frac{\partial}{\partial \tau_j} \sum_{i=1}^N \frac{\lambda_i}{\lambda_{max}} \cdot \log \left[\frac{1}{T_{av}} \tau_i \prod_{\substack{k=1 \\ k \neq i}}^N (1 - \tau_k) (1 - P_e^{(i)}) PL^{(i)} \right] = \\
& \frac{\partial}{\partial \tau_j} \sum_{i=1}^N \frac{\lambda_i}{\lambda_{max}} \cdot \left[\log \tau_i + \sum_{\substack{k=1 \\ k \neq i}}^N \log(1 - \tau_k) + \log(1 - P_e^{(i)}) + \right. \\
& \qquad \qquad \qquad \left. + \log(PL^{(i)}) - \log(T_{av}) \right] = \\
& \frac{\partial}{\partial \tau_j} \sum_{i=1}^N \frac{\lambda_i}{\lambda_{max}} \cdot \left[\log \tau_i + \sum_{\substack{k=1 \\ k \neq i}}^N \log(1 - \tau_k) - \log(T_{av}) \right] \tag{26}
\end{aligned}$$

whereby the last relation stems from the independence of $P_e^{(i)}$ and $PL^{(i)}$ on τ_j . Exchanging the derivative with the summation yields:

$$\frac{\lambda_j}{\lambda_{max}} \frac{1}{\tau_j} - \frac{1}{1 - \tau_j} \sum_{k=1, k \neq j}^N \frac{\lambda_k}{\lambda_{max}} - \frac{C}{T_{av}} \frac{\partial T_{av}}{\partial \tau_j}, \quad \forall j = 1, \dots, N \tag{27}$$

whereby $C = \sum_{i=1}^N \frac{\lambda_i}{\lambda_{max}}$. By equating (27) to zero, (24) easily follows.

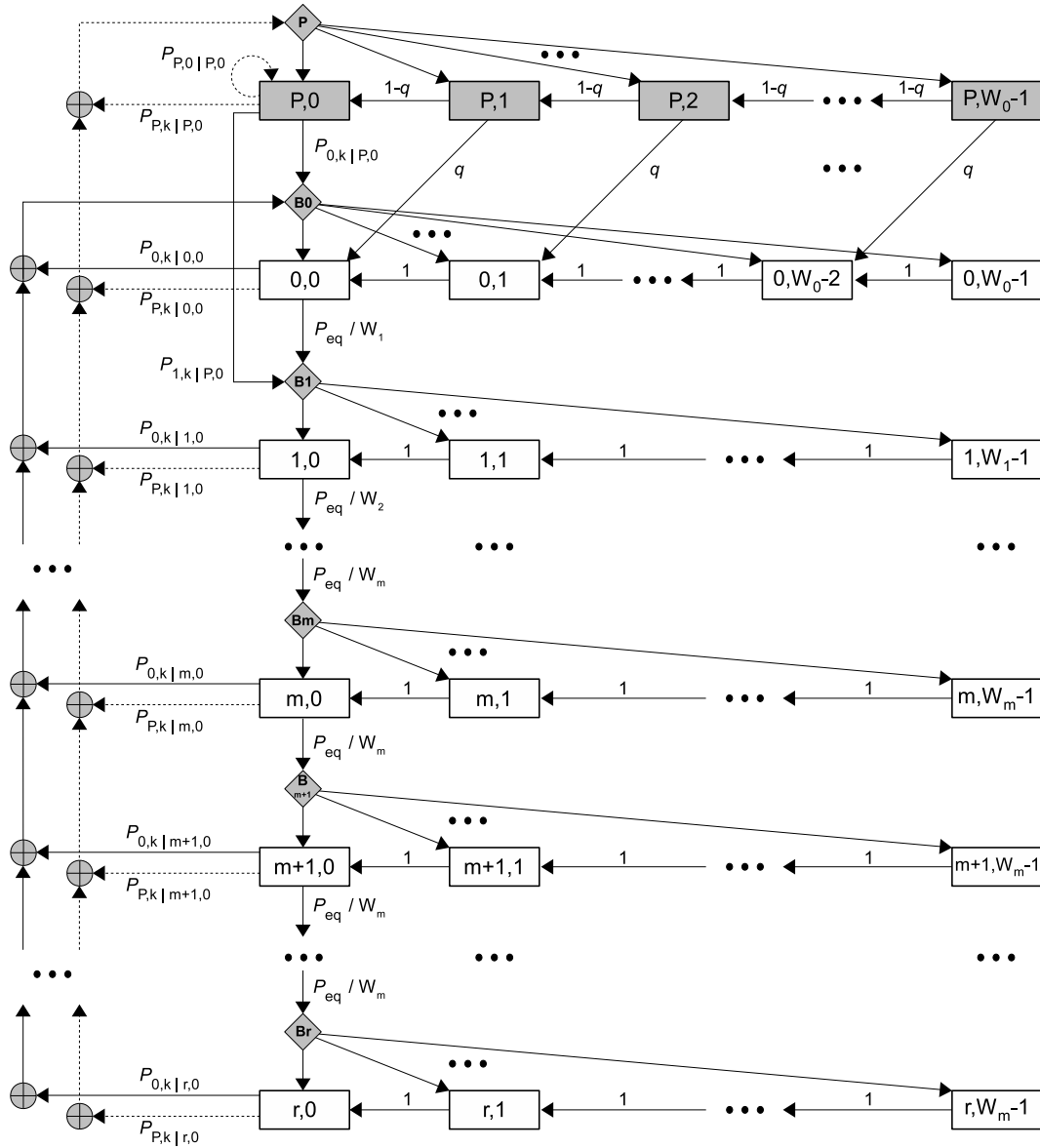


Fig. 1. Markov chain for the contention model of the generic s -th station in general traffic conditions, based on the 2-way handshaking technique, considering the effects of channel induced errors, unloaded traffic conditions, and post-backoff.

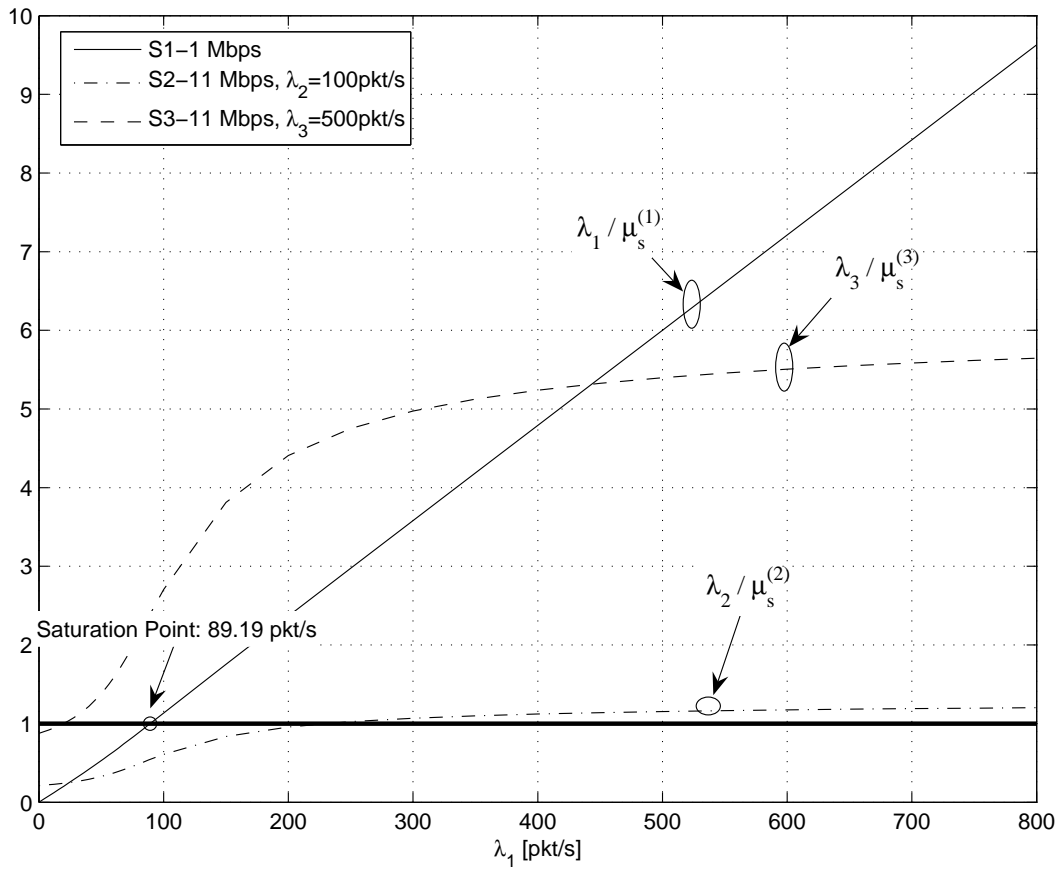


Fig. 2. Behaviour of the ratio $\lambda_t / \mu_s^{(t)} = \lambda_t \cdot T_{serv}^{(t)}$ in (19) in a network of three contending stations (labelled S1, S2 and S3) as a function of the packet rate λ_1 of the slowest station S1 transmitting at 1 Mbps. The other two stations transmit at 11 Mbps with constant packet rates, respectively equal to 100pkt/s and 500pkt/s. The packet size PL is equal to 1028 bytes for the three contending stations.

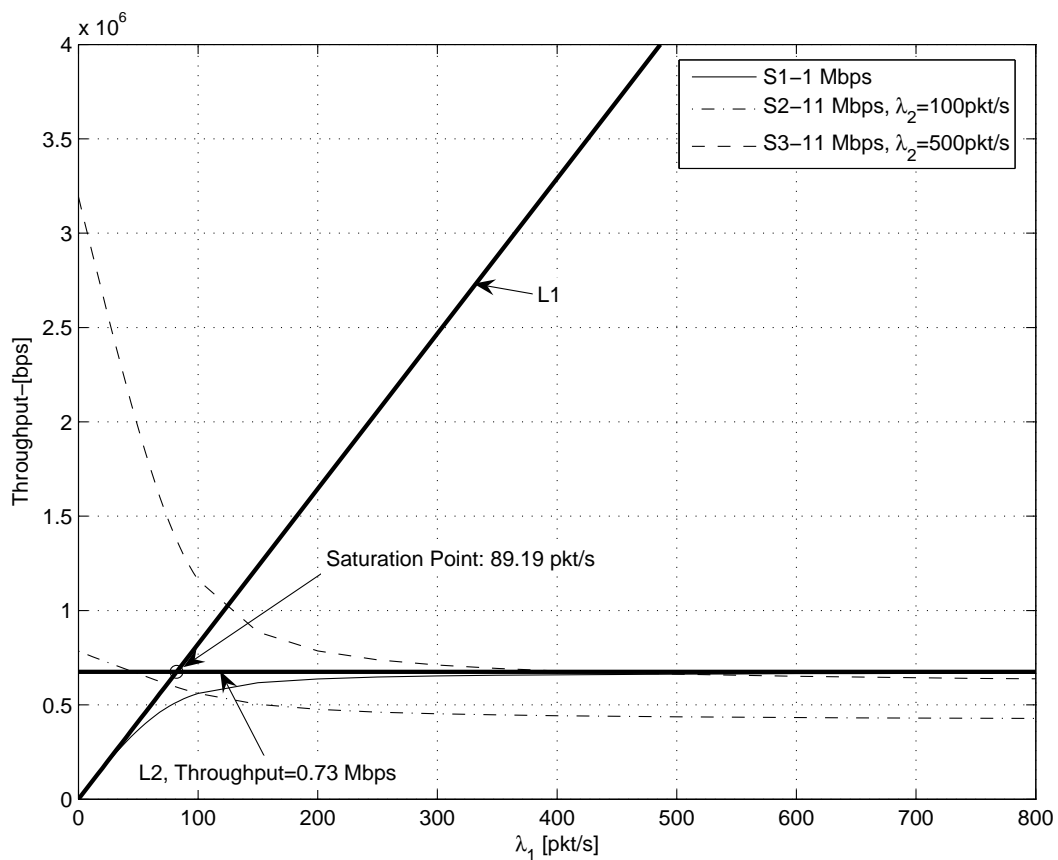


Fig. 3. Behaviour of the per-station throughput in a network of three contending stations (labelled S1, S2 and S3) as a function of the packet rate λ_1 of the slowest station S1 transmitting at 1 Mbps. The other two stations transmit at 11 Mbps with constant packet rates, respectively equal to 100pkt/s and 500pkt/s. The packet size PL is equal to 1028 bytes for the three contending stations.

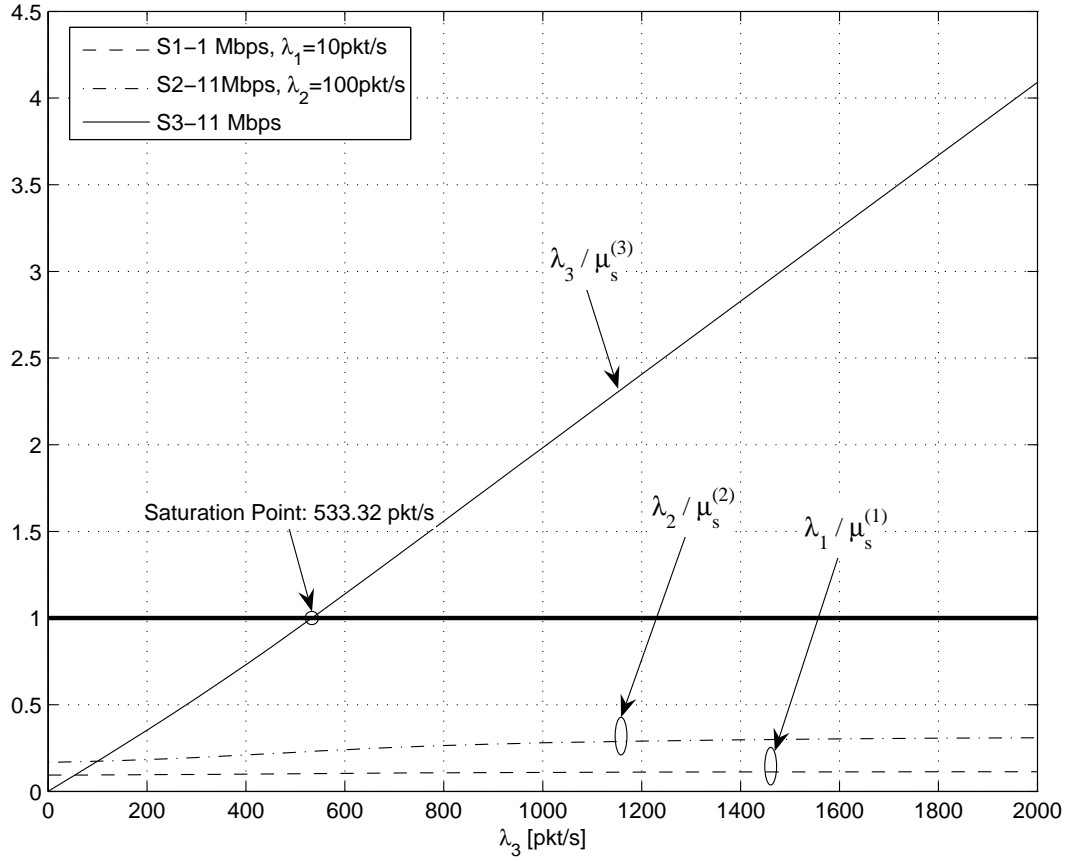


Fig. 4. Behaviour of the ratio $\lambda_t / \mu_s^{(t)} = \lambda_t \cdot T_{serv}^{(t)}$ in (19) in a network of three contending stations (labelled S1, S2 and S3) as a function of the packet rate λ_3 of the fastest station S3 transmitting at 11 Mbps. The station S1 transmits with constant packet rate 10pkt/s at 1 Mbps, whereas the station S2 transmits with constant packet rate 100pkt/s at 11 Mbps. The packet size PL is equal to 1028 bytes for the three contending stations.

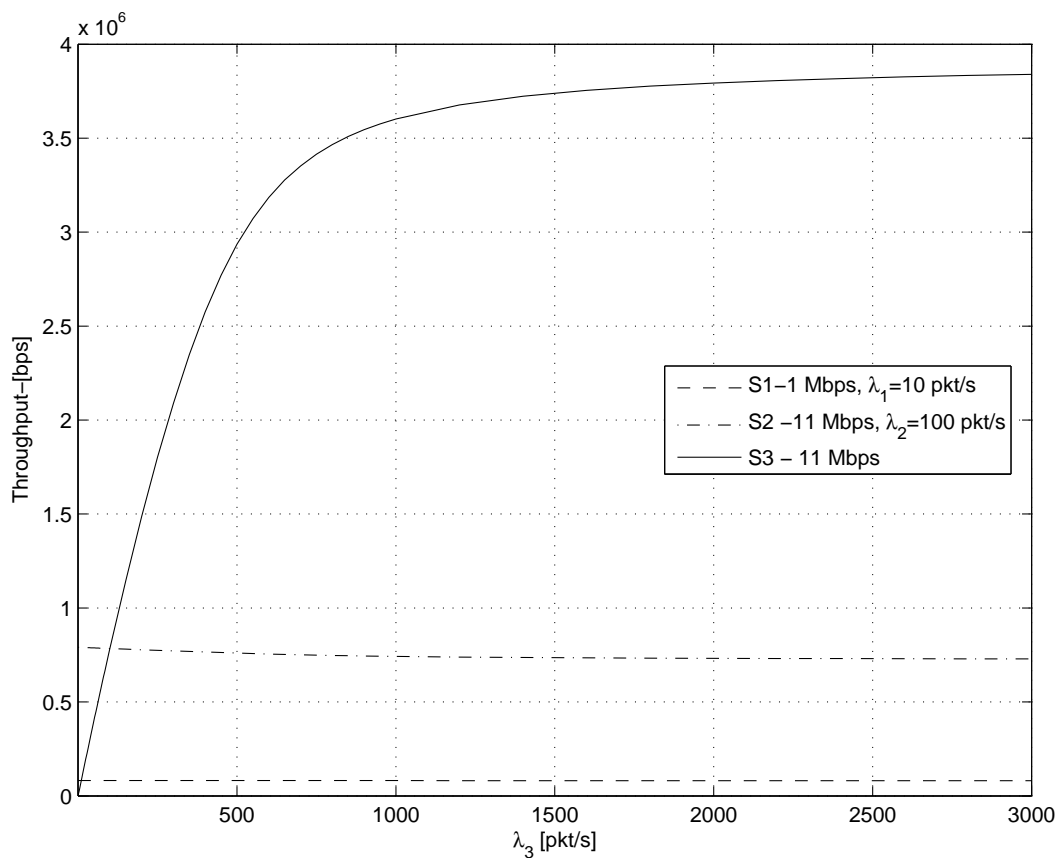


Fig. 5. Behaviour of the per-station throughput in a network of three contending stations (labelled S1, S2 and S3) as a function of the packet rate λ_3 of the fastest station S3 transmitting at 11 Mbps. The other two stations transmit with constant packet rates, respectively equal to 10pkt/s and 100pkt/s. The packet size PL is equal to 1028 bytes for the three contending stations.

TABLE I
TYPICAL NETWORK PARAMETERS

MAC header	28 bytes	Propag. delay τ_p	1 μs
PLCP Preamble	144 bit	PLCP Header	48 bit
PHY header	24 bytes	Slot time	20 μs
PLCP rate	1Mbps	W_0	32
No. back-off stages, m	5	W_{max}	1024
Payload size	1028 bytes	SIFS	10 μs
ACK	14 bytes	DIFS	50 μs
ACK timeout	364 μs	EIFS	364 μs

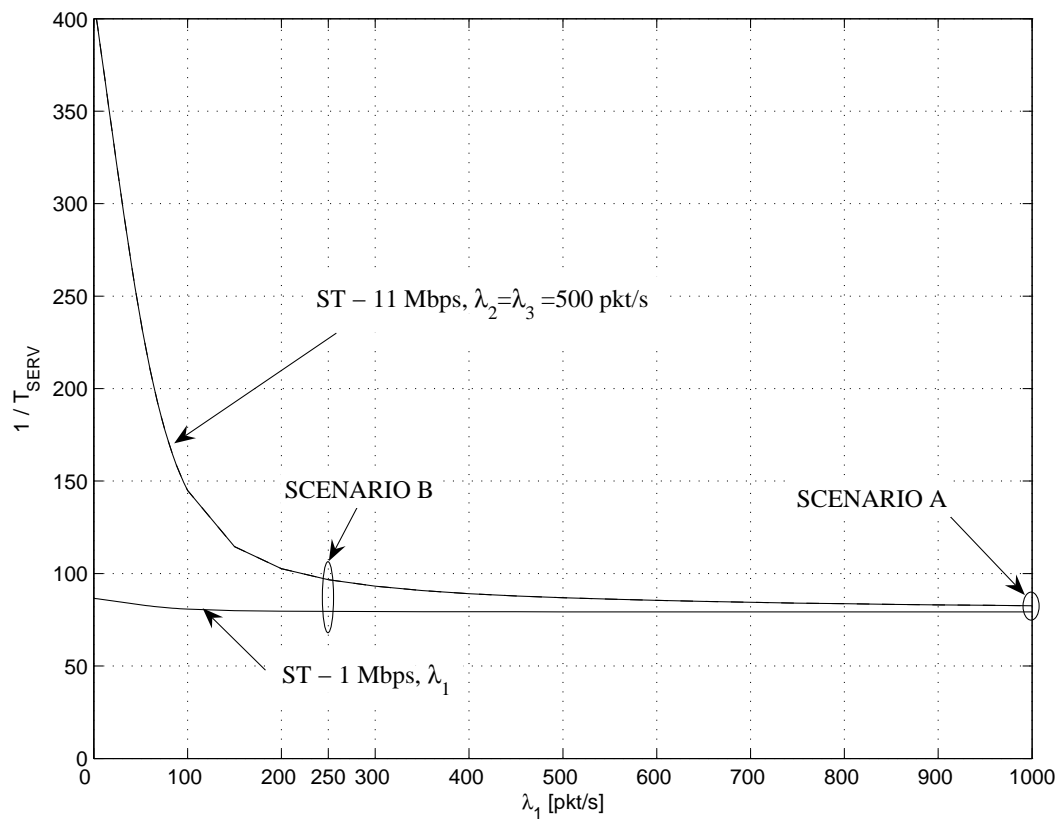


Fig. 6. Behaviour of the critical packet rates ($\mu_S^{(t)} = 1/T_{serv}^t$) in a network of three contending stations as a function of the packet rate λ_1 of the slowest station transmitting at 1 Mbps. The other two stations transmit with a constant packet rate equal to 500pkt/s at 11 Mbps. Notice that curves $\mu_S^{(t)}$ related to the stations at 11 Mbps are superimposed since they both employ the same network parameters.

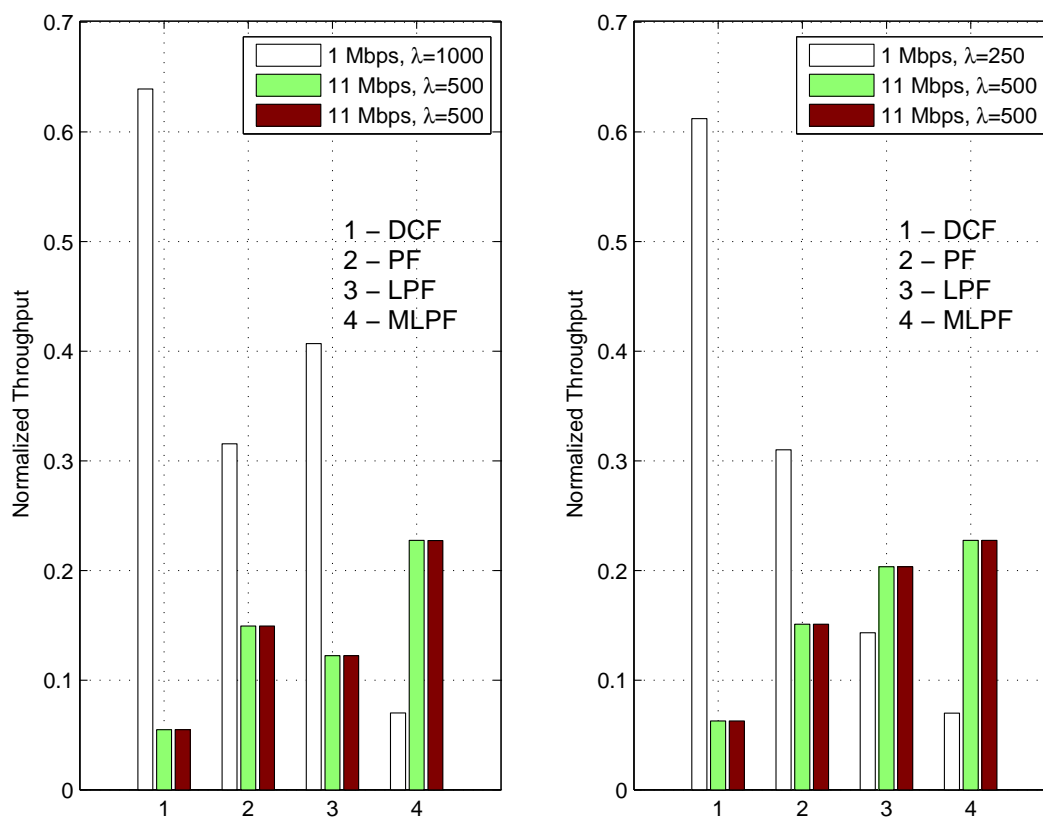


Fig. 7. Simulated normalized throughput achieved by three contending stations upon employing 1) a classical DCF; 2) DCF with PF allocation; 3) DCF optimized as noted in (23); and 4) DCF optimized with the MLPF criterion. Left and right plots refer to scenarios A and B, respectively.

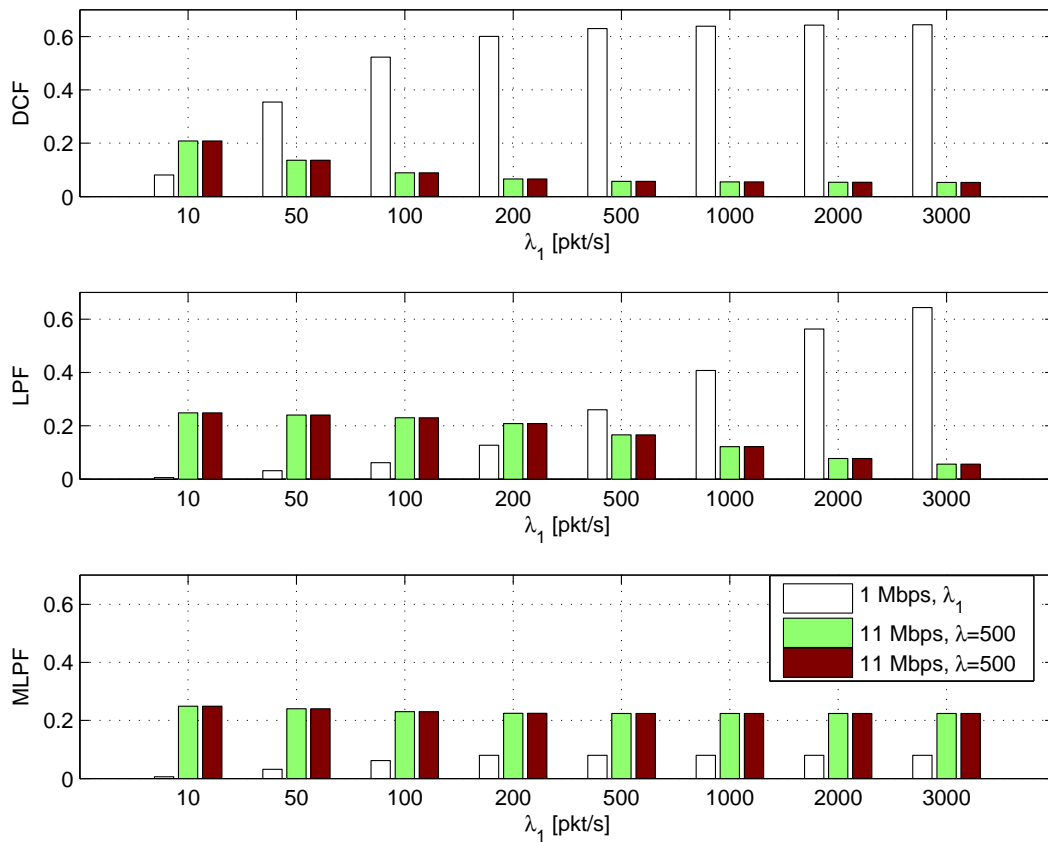


Fig. 8. Simulated normalized throughput achieved by three contending stations as a function of the packet rate of the slowest station in DCF, LPF and MLPF modes.